

A comparative study of digital low dropout regulators

Mo Huang^{1, †}, Yan Lu¹, and Rui P. Martins^{1,2}

¹State Key Laboratory of Analog and Mixed-Signal VLSI, Institute of Microelectronics, DECE/FST, University of Macau, Macau, China

²On leave from the Instituto Superior Técnico, Universidade de Lisboa, Lisbon, 1049-001, Portugal

Abstract: Granular power management in a power-efficient system on a chip (SoC) requires multiple integrated voltage regulators with a small area, process scalability, and low supply voltage. Conventional on-chip analog low-dropout regulators (ALDOs) can hardly meet these requirements, while digital LDOs (DLDOs) are good alternatives. However, the conventional DLDO, with synchronous control, has inherently slow transient response limited by the power-speed trade-off. Meanwhile, it has a poor power supply rejection (PSR), because the fully turned-on power switches in DLDO are vulnerable to power supply ripples. In this comparative study on DLDOs, first, we compare the pros and cons between ALDO and DLDO in general. Then, we summarize the recent DLDO advanced techniques for fast transient response and PSR enhancement. Finally, we discuss the design trends and possible directions of DLDO.

Key words: low dropout regulator (LDO); digital control; fast transient response; power supply rejection (PSR); integrated voltage regulator

Citation: M Huang, Y Lu, and R P Martins, A comparative study of digital low dropout regulators[J]. *J. Semicond.*, 2020, 41(11), 111405. <http://doi.org/10.1088/1674-4926/41/11/111405>

1. Introduction

Resources in system-on-a-chip (SoC) are highly dynamic. Fig. 1 shows, under different workloads, resources such as execution units (EUs), fixed functions (FFs), and media units that can be in high demand, low demand, or retention modes. Therefore, for good system energy efficiency, we should use individual supply voltage domains for these units, each with a voltage regulator, a. k. a. granular power management^[1,2]. Candidates for the regulator are the DC–DC converter and the low-dropout regulator (LDO). Although LDO suffers from an inherently lower efficiency than that of the DC–DC converter (100% in an ideal case), it is more compact with the removal of large energy storage components (inductors, capacitors) and hence suitable to obtain a fully-integrated voltage regulator (FIVR) in an SoC. Besides, a fully-integrated LDO reacts swiftly to the load transients for its light-weight nature (with a single-pole power stage).

However, for an energy-efficient SoC, the load circuits may operate at a near-threshold supply voltage like 0.5 V, while the dropout voltage should be small, for example 50 mV. These working conditions hardly suit analog LDOs (ALDOs)^[3–9], which need sufficient voltage headroom to realize a high loop gain to minimize the steady-state error of the output voltage. Alternatively, we may use the multistage topologies to increase the loop gain, but complicated frequency compensation techniques are then necessary.

On the other hand, digital LDOs (DLDO) are a good alternative^[10–41] for a power-efficient SoC. The digitized power transistors of the DLDO work like switches, allowing a small dro-

pout voltage (Fig. 2). Also, we can easily implement a high loop gain with a digital integrator that is not limited by the minimum supply voltage (V_{MIN}).

The widely-adopted shift-register-based DLDO firstly proposed in Ref. [10], included a power switch array, a clocked comparator to sense the output and the reference voltage difference, plus a shift-register (acting as an integrator) to generate a control word of the power switch array. Yet the synchronized shift-register only changes the control word by 1-bit every clock cycle, and thus only a high-frequency clock will allow a fast response. This increases the power consumption of the synchronized circuits. To address this trade-off, many techniques have been proposed, they will be addressed and discussed in this paper.

Another issue faced by DLDO is the power supply rejection (PSR). Fig. 2 illustrates how the load current change from a neighbor load may cause voltage ripple on the shared DLDO input. Also, input ripple can come from the pre-stage DC–DC converter. Unfortunately, the PSR of the DLDO is inherently inferior to that of the ALDO, especially when we maintain the control clock as low under the power consumption constraint. As a result, significant ripples may also occur at the DLDO output node. To prevent abnormal/interrupt operations of the load circuits caused by these supply ripples, implies the addition of a margin above the minimum workable supply voltage V_{MIN} , which undermines the efficiency. Therefore, this paper will also investigate PSR enhancing techniques for DLDO^[32–35].

This paper has the following organization: Section 2 discusses the pros and cons of the ALDO and the DLDO. Section 3 reviews the DLDO techniques on how to minimize output voltage spike, recovery time, and improve PSR. Section 4 presents the possible future trends of the DLDO design, and draws the conclusion.

Correspondence to: M Huang, mohuang@um.edu.mo

Received 25 JULY 2020; Revised 26 SEPTEMBER 2020.

©2020 Chinese Institute of Electronics

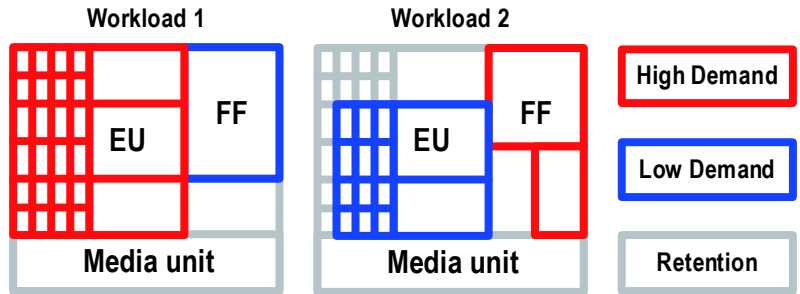


Fig. 1. (Color online) Granular power management in an SoC.

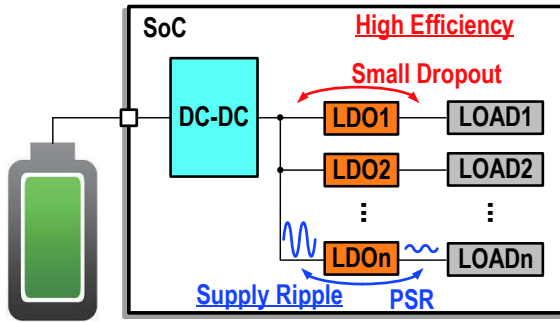


Fig. 2. (Color online) DLDO requirements in an SoC.

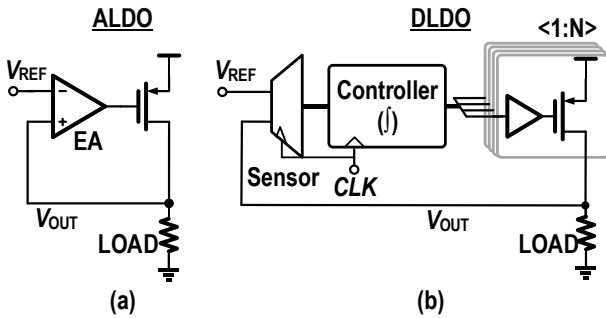


Fig. 3. Block diagram of (a) ALDO and (b) DLDO.

2. Comparison between analog and digital LDOs

2.1. Low voltage operation and process scalability

Fig. 3 presents the basic block diagrams of the ALDO and the DLDO. The ALDO compares the output voltage (V_{OUT}) with the reference voltage (V_{REF}) through an error amplifier (EA). The EA's output feeds a power transistor that operates in the saturation region in most of the cases, although it sometimes operates in the linear region as well. To maintain good output accuracy, the ALDO should have an EA with sufficient loop gain. To circumvent the stability issue of a multistage system, it would be necessary to have a one- or two-stage EA with cascode devices. Yet, more cascode devices stacked imply a larger voltage headroom, which limits the minimum supply voltage of an energy-efficient SoC. Moreover, the analog EA has a weak process scalability, and requires re-design in process migration.

The DLDO replaces the analog EA by a V_{OUT} sensor and a controller (integrator) implemented with digital circuits. The digital integrator manages to provide a very high DC gain that is irrelevant to its supply voltage, breaking the trade-off between loop gain and supply voltage in the analog design. As such, DLDO works well with a low supply voltage, and

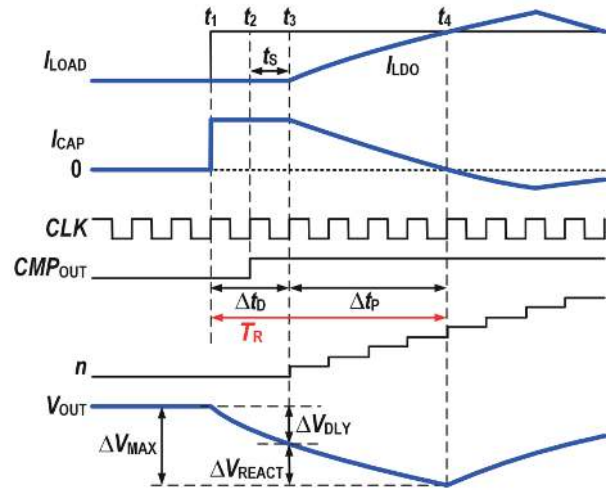


Fig. 4. (Color online) The output voltage undershoot analysis of DLDO.

scales naturally with an advanced process. Meanwhile, the switch operation of the power transistors conducts more current with a full turn-on voltage (V_{DD}), saving silicon area.

In recent years, the inverter-based LDO^[42–44] stems from the ring amplifier, for low-voltage operation. They achieve a fast response with the inverters working in an analog fashion. However, to reduce shoot-through currents in the inverters, offset voltages should exist for proper biasing. Obviously, during process migration, the offset voltages require a dedicated calibration circuit, otherwise, re-design is necessary.

2.2. Power-speed trade-off

The widely adopted figure of merit (FoM) of speed proposed in Ref. [45] explains the power-speed trade-off of LDO:

$$FOM = T_R \frac{I_Q}{I_{MAX}} = \frac{C_{OUT} \cdot \Delta V_{OUT}}{I_{MAX}} \cdot \frac{I_Q}{I_{MAX}}, \quad (1)$$

where T_R is the transient response time, I_Q is the quiescent current, I_{MAX} is the maximum load current, C_{OUT} is output capacitor, and ΔV_{OUT} is the output voltage spike with the I_{MAX} load step.

For an ALDO, T_R is mainly determined by the bandwidth of the LDO loop and slew rate, which should be inversely proportional to the I_Q . Multiple-loop schemes could be a good way to reduce T_R without significantly increasing I_Q [4, 46].

The synchronous DLDO should have a longer T_R and thus a slower transient response under the I_Q constraint, due to the conventionally discrete V_{OUT} sampling and synchronized control word changing, as illustrated in Fig. 4. When a load cur-

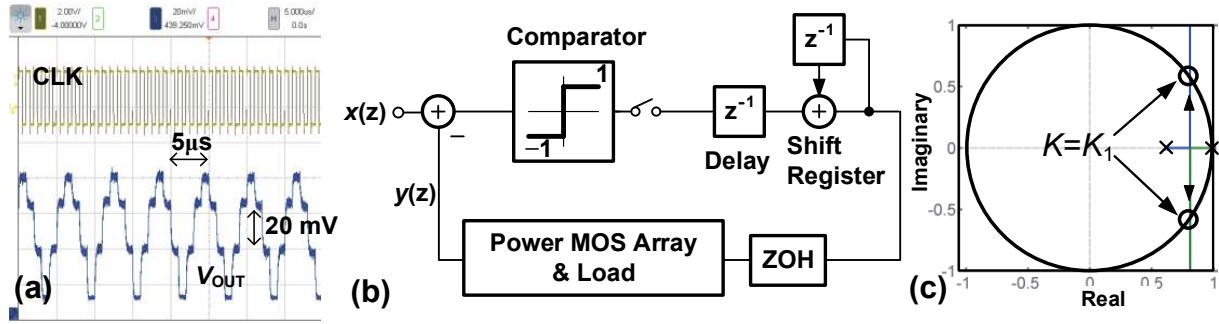


Fig. 5. (a) Measured LCO of DLDO, (b) small-signal model of DLDO, and (c) root locus of 2-level quantized DLDO.

rent (I_{LOAD}) step comes at t_1 , DLDO fails to respond instantly. The output capacitor compensates the difference between I_{LOAD} and LDO output current I_{LDO} , leading to a V_{OUT} drop, until the next clock (CLK) rising edge (t_2) when the synchronized comparator can respond. To prevent metastability, the controller, lagging one-cycle behind t_2 (t_3), processes the comparator's output (CMP_{OUT}). After that, the control word n begins to increase, providing additional current I_{LDO} . We define $\Delta t_D = t_3 - t_1$ as the loop delay, and V_{OUT} the undershoot caused by Δt_D is ΔV_{DLY} . Subsequently, V_{OUT} does not stop decreasing until $I_{LDO} = I_{LOAD}$, depending on how fast the controller can find the desired control word within the processing time (Δt_p). This adds an additional voltage drop ΔV_{REACT} to the overall undershoot $\Delta V_{MAX} = \Delta V_{DLY} + \Delta V_{REACT}$. Consequently, the T_R of the DLDO consists of Δt_D and Δt_p , where only Δt_p contributes to the T_R in analog counterparts.

Due to the discrete sampling, the maximum Δt_D is two-clock cycle. Hence under the power consumption constraint, ΔV_{DLY} of the DLDO would be larger than that of the ALDO. To reduce Δt_D , continuous or asynchronous sampling techniques emerged, presented next in Section 3.

To reduce ΔV_{REACT} , many recent DLDO techniques tried to find out the desired control word within a few cycles, taking the advantage of digital operations (discussed in Section 4). This imposes the DLDO to have a comparable or even smaller ΔV_{REACT} than the ALDO.

2.3. Stability and limit cycle oscillation

For conventional ALDO designs, an ALDO will become unstable or even oscillate once its phase margin is not enough. But regarding the DLDO, which typically has a DC pole from the digital integrator, large signal unstable behaviour is less likely to happen. However, DLDOs suffer from another oscillation phenomenon inexistent in ALDOs. Because of the digitized output current with limited resolution, there will always be a quantization error in the DLDO, inciting a limit cycle oscillation (LCO).

The quantization level determines the quantization error. Fig. 5(a) displays a measured V_{OUT} LCO waveform of a two-level quantized DLDO^[11], with a period of integer clock cycles and an amplitude of several milli-volt. Refs. [12, 13] explain the difference between an LCO and oscillation in analog circuits, with the small-signal model of a two-level quantized DLDO in Fig. 5(b). With a DC pole and an output pole, Fig. 5(c) plots the root locus of this system. The LCO appears when the root locus crosses the unit circle (a "healthy" oscillation). By contrast, the analog loop instability basically occurs outside the unit circle. Ref. [11] further investigated a meth-

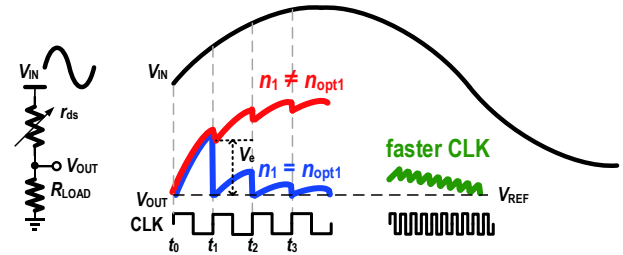


Fig. 6. (Color online) Power supply rejection process of a conventional DLDO.

od to predict the period and amplitude of the LCO.

Generally speaking, a smaller least significant bit (LSB) current reduces the quantization error and subsequently the LCO. Nonetheless, the small LSB exponentially increases the control bits required for the targeted output current. A pulse-width-modulated (PWM) LSB scheme proposed in Ref. [14] reduces the effective LSB. Additionally, Ref. [11] added an auxiliary path to reduce the LCO mode to 1 across a wide load current range.

2.4. Power supply rejection

An ALDO can achieve a good PSR with a properly designed EA and a dominant pole allocation^[4, 9], or by adding a feedforward path to cancel the supply input ripple^[7]. But the low supply and dropout voltages in an energy-efficient SoC inevitably undermine the achievable PSR.

Fig. 6 illustrates the power supply ripple rejection process of a DLDO, where discontinuous sampling and control word changing will excite significant glitches with a supply voltage ripple. We define the optimum control word n (n_{opt}) that imposes $V_{OUT} = V_{REF}$ in the steady-state, with the change of n synchronized with the clock rising edge. In an ideal case, the controller manages to find out n_{opt} ($n_1 = n_{opt}$) at each sampling point (t_0, t_1, t_2, t_3), with V_{OUT} pulled-back to V_{REF} . However, during the sampling intervals, e.g., from t_0 to t_1 , with n fixed, the instant PSR becomes:

$$PSR = \frac{1}{1 + \frac{R_{LOAD}}{r_{ds}}}, \quad (2)$$

where r_{ds} represents the instance resistance of the power transistor (constant value during the intervals), R_{LOAD} is the load resistance. This indicates that the DLDO is vulnerable to the supply ripple during the sampling intervals.

For the non-ideal cases when $n_1 \neq n_{opt}$, e.g., at t_1 , it causes an error $V_e = V_{OUT} - V_{REF}$. Then before the next sam-

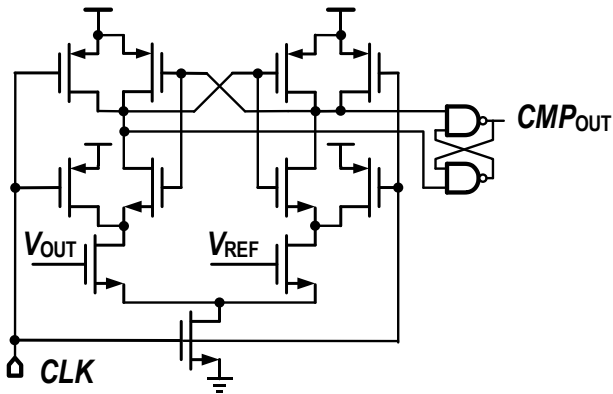


Fig. 7. Latch-based comparator.

pling, V_{OUT} starts to increase with V_{IN} from V_e , leading to a larger V_{OUT} ripple. Therefore, the only way for a conventional DLDO to improve the PSR is to minimize the sampling interval using a faster CLK. Unfortunately, this contradicts the power-efficient prerequisite. Section 5 introduces several techniques to incorporate a continuous analog path to enhance the PSR.

3. Design considerations about the DLDO

3.1. Quantizer

A quantizer will approximate the voltage error between V_{OUT} and V_{REF} for further processing. Conventional DLDOs use a two-level, synchronized, latch-based comparator^[2, 10, 13, 15–18], as shown in Fig. 7, quantizing V_{OUT} to a binary output. The complementary clock-controlled switches in the comparator eliminate the steady quiescent current. However, the clock limits the quantization speed, and the discontinuous sampling causes a certain delay Δt_D . Meanwhile, the unbalanced parasitic capacitance and transistor mismatches will cause input offset^[19].

High-performance DLDO designs^[20–23] use continuous quantization, typically achieved with a multi-level quantization (functioning as an analog-to-digital converter, ADC). In Ref. [21], a transconductance stage continuously compares V_{OUT} and V_{REF} , and a current-to-code converter generates a multi-bit output (Fig. 8(a)). A code-dependent reference increases the dynamic range and resolution of the converter. Ref. [22] designed a continuous quantizer also based on inverters, as shown in Fig. 8(b). An auto-zero technique removes the input offset voltage of the aforementioned inverter-based analog LDO. A time-to-digital converter (TDC) is another candidate for continuous multi-level quantization^[23], but needs calibration on the delay time. Plus, the quantized multi-level signals processed by digital logic lead to a more coherent DLDO. But in general, the power consumption of the multi-level quantizer is much higher.

A voltage-controlled oscillator (VCO) can also be a continuous quantizer^[24, 25]. Fig. 9 shows how with the two VCOs driven by V_{OUT} and V_{REF} , the DLDO system looks like a phase-locked loop (PLL). In the steady-state, the VCOs should oscillate at the same frequency, resulting in a fixed phase error subsequently converted to a control word by the phase detector (PD). When a load current step occurs, the V_{OUT} spike information turns into an incremental phase error, captured by the PD and processed by the controller. The main drawback of

this topology is that the VCO is essentially an integrator ($1/s$), that needs enhancement of the transient speed by a proportional control, as presented next.

As a brief summary, the features of the quantizers in DLDO design are included in Table 1.

3.2. PID control

One of the possible solutions to address the power-speed trade-off of the DLDO is to use asynchronous control logic^[26, 27], but the asynchronous design may not be robust under process, voltage, temperature (PVT) variations.

Another straightforward way combines the proportional, integral (PI), and even derivative (PID) controls^[28] for better transient response. Fig. 10 displays the conceptual transient waveforms of these controls. For a conventional I-control that has a large DC gain, DLDO achieves an accurate steady-state output but low speed. By contrast, P-control can minimize V_{OUT} undershoot, but lacks the capability of reducing the steady-state error. PI-control can address both drawbacks, while PID-control further suppresses the recovery overshoot.

3.2.1. Digital PID control

As discussed above, the number of the quantization levels should be proportional to the power consumption. For a low power design, the detection of whether V_{OUT} exceeds the V_{REF} window^[2, 13] can activate the P-control, namely a three-level quantization. Fig. 11 presents the comparison of V_{OUT} in two comparators, with V_{REFH} and V_{REFL} , respectively, forming a $V_{REFH} - V_{REFL}$ window. When V_{OUT} exceeds this window, the sampling frequency increases with P-control, driving V_{OUT} back to the window quickly. When it is within the window, the comparison of V_{OUT} with V_{REF} generates the control word after the integrator, as an I-control.

High-performance designs employ typically a multi-level quantization with an ADC^[14, 20–22]. With the V_{OUT} information converted to the digital domain, the control circuits can perform easily the PID control. However, to reduce the loop delay, a power-hungry ADC may be necessary.

Granular power management oversees not only the V_{OUT} overshoot/undershoot, but also the recovery time. For a linear increment control used in the conventional DLDO^[10], the control word can only change one count per clock cycle, resulting in a very long recovery time. The coarse-fine tuning scheme used in Refs. [2, 13, 29], changes the control word in multiple counts per clock cycle (coarse-tuning) once V_{OUT} exceeds the predefined window. A more aggressive scheme utilizes binary search with the control word changing with 2^M ^[14], with D-control added to prevent a recovery overshoot. To reduce the overshoot without D-control, Ref. [30] used exponential control expressed as:

$$(W/L)_n = \text{Const.} \times q^n, \quad q > 1, \quad (3)$$

where the recovery time may be a bit longer than the binary search.

3.2.2. Analog-assisted loop

By using analog circuits to sense V_{OUT} ^[15–18, 31] as the fast loop can also be a candidate, due to the continuous nature of the analog circuits. Meanwhile, it is worthwhile to utilize passive devices, as active circuits may still have limitations in terms of their low supply voltage and small dropout.

Fig. 12(a) presents an “analog-assisted” method propo-

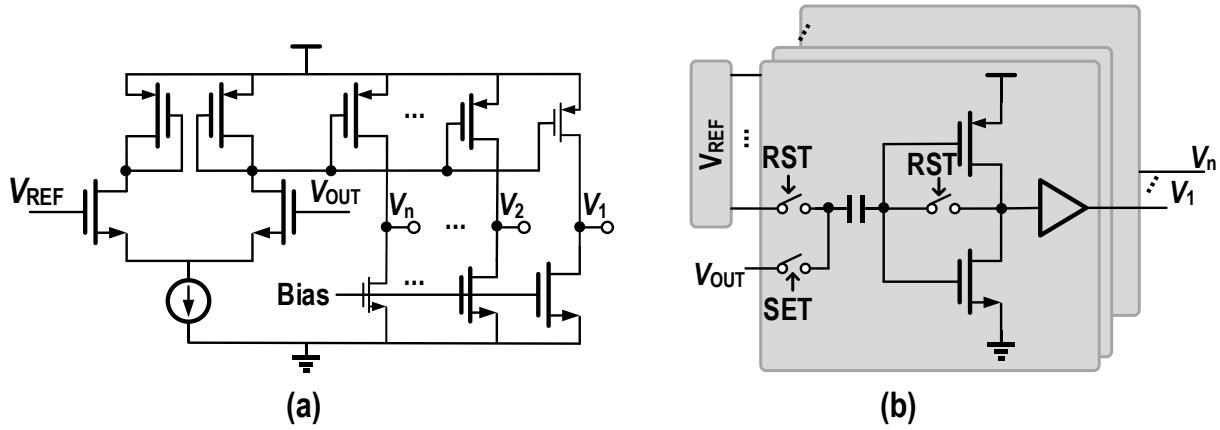


Fig. 8. Continuous multi-bit quantizer based on (a) current-mirror and (b) inverter.

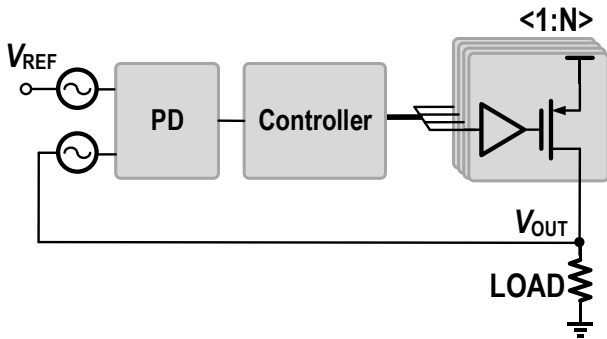


Fig. 9. DLDO based on a VCO quantizer.

sed in Refs. [15, 16]. A passive high-pass network R_C and C_C couples to the ground of the driving inverters (V_{SSB}) the high-frequency components of V_{OUT} . R_C biases V_{SSB} to the ground in the steady-state, while drops to a negative value (almost equal to the V_{OUT} undershoot) at the load transient with a minor delay, allowing the power transistors to generate more instantaneous output current as a high-pass path. Ref. [17] further reduces the V_{OUT} undershoot by providing more instantaneous current, through coupling V_{OUT} to the body of the power transistors. The drawback of these schemes is that the analog circuit can only assist the turned-on power transistors, setting a limit on the minimum output current. Ref. [18] proposed an improved version (Fig. 12(b)), where analog paths include not only the high-pass network (P_2), but also NMOS pass devices (P_1). This advances the PMOS counterpart, by providing more instantaneous current from both turned-on and -off pass devices. Nevertheless, this benefit trades with the need for a gate drive voltage higher than the supply voltage. Ref. [31], although not implemented from a digitized output power transistor array, also utilizes a capacitor to couple the output spike to the gate of the power transistor as a high-pass path (Fig. 12(c)). A charge pump generates the gate voltage of the power transistor. Though it is analog in nature, it can be a good candidate for a low-power DLDO.

In addition, the analog-assisted methods can be an effective solution to improve the DLDO transient response without using advanced process. Table 2 summarizes the process nodes and FoMs (from (1)) of state-of-the-art DLDO works, to evaluate how the process advancement enhances the DLDO performance. As can be seen, the FoM value decreases with process scaling down for the ADC-based DLDO designs [21, 22, 36, 39, 40]. This stems from the fact that the ADC

and digital processing has a higher speed and better power efficiency with advanced process. Yet, it is interesting to find out that the analog-assisted-based DLDOs [15, 18] manage to achieve even better FoMs with a cost-effective process, which is facilitated by the continuous response of the analog circuits.

3.3. PSR improvements

As discussed in Section 2, the DLDO has inherently mediocre PSR even when the optimum control word can be found. Instead, analog circuits may be the only solution under the power consumption constraint. As illustrated in Fig. 13(a), by parallelizing an analog resistance $r_{ds,A}$ with the digitized resistance $r_{ds,D}$, the overall resistance can change continuously. Additionally, feedback loops may adjust $r_{ds,A}$ from the supply voltage noise, just like in the ALDO. Then, with the supply voltage V_{IN} -to- V_{OUT} response mainly determined by the analog circuits, they allow a longer digital sampling interval (t_4 to t_5), and thus higher power consumption. Fig. 13(b) exhibits a topology that combines analog and digitized resistance classified as an hybrid LDO [32].

Although the working principle of the PSR improving techniques in the digital/hybrid LDO are similar to those in the ALDO, there are two critical issues remaining. Firstly, we expect the current provided by the analog part to be small. Hence even with a continuously adjustable $r_{ds,A}$, this LDO fails to respond to a large supply ripple. Secondly, the limited supply voltage and dropout undermine the achievable PSR of the analog circuits.

Ref. [33] employed one ALDO array and one DLDO array, and proposed a feedforward PSR cancellation technique (Fig. 14(a)), implemented with a resistor and capacitor between the supply voltage and the gate node of the power transistor. It improves the light-load PSR, degraded at heavy load. To maintain the PSR performance, the architecture should comprise more ALDOs and less DLDOs under heavy load conditions.

As presented in Fig. 14 (b), Refs. [34, 35] added an active replica loop to enhance the PSR. The main part of the ALDO constructed from a flipped voltage follower (FVF) [4, 5] (M_{PA} , M_2 , A_1), manages to work under a low supply voltage with a fast transient response. Fig. 15 plots the simulated PSR, showing a significant improvement above 10 kHz, when compared with a conventional DLDO. The addition of the replica loop, composed by M_{Pr} , M_{2r} , and A_2 , increases the loop gain

Table 1. Features of the quantizers in DLDO design.

Type		Continuous Sensing	Speed	Power Consumption	Robustness
Single-bit		No	Fast	Low	High
Multi-bit	Current-to-code ADC ^[21]	Yes	Fast	High	High
	Flash ADC ^[22]	Yes	Fast	High	High
	TDC ^[23]	Yes	Fast	Medium	Need calibration
	VCO+PD ^[24, 25]	Yes	Slow (1/s effect)	Medium	High

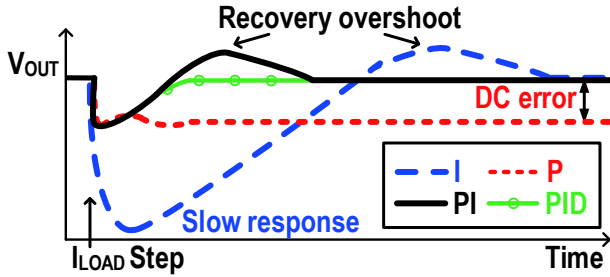


Fig. 10. (Color online) Output voltage transient response under I-only, P-only, PI, and PID control.

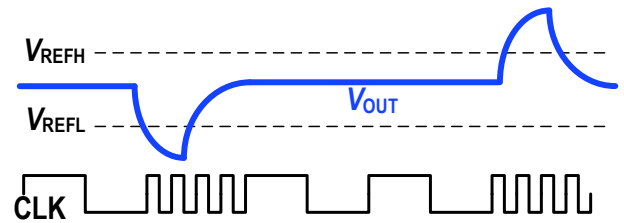


Fig. 11. Change CLK when V_{OUT} exceeds the V_{REF} window.

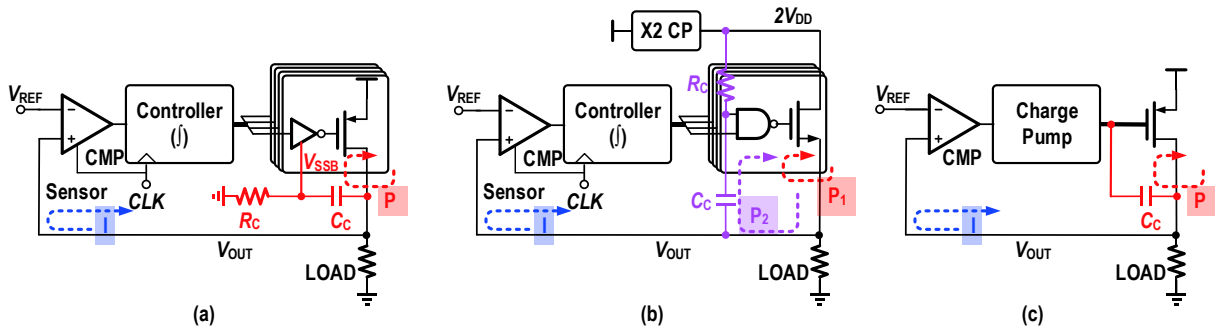


Fig. 12. (Color online) Analog-assisted loop in (a)^[15–17], (b)^[18], and (c)^[31].

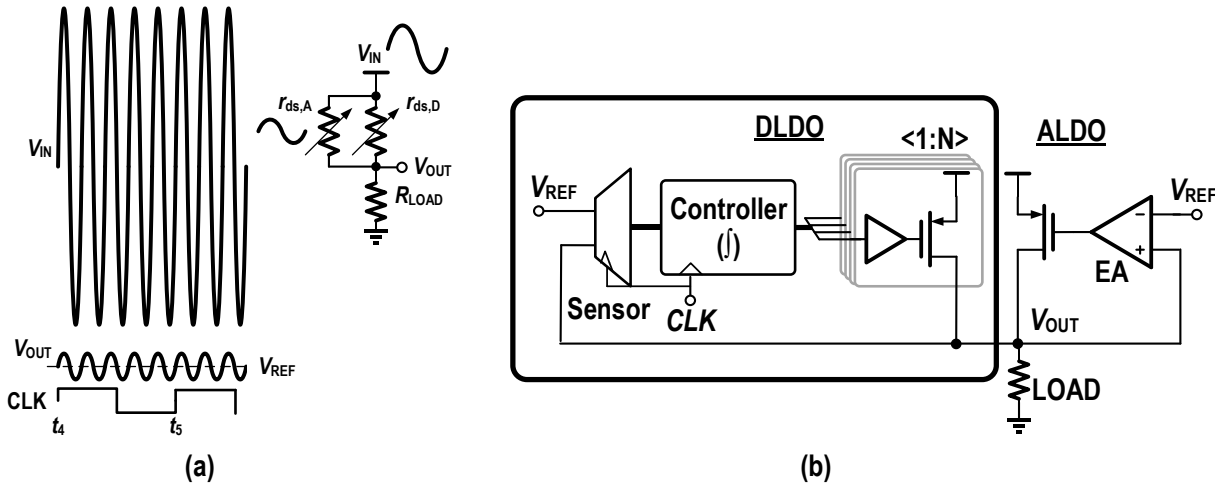


Fig. 13. (a) Analog circuits help PSR improvement and (b) block diagram of the hybrid LDO.

and then improves the PSR by 6 dB (5.3 in simulation). Additionally, the current provided by the ALDO dynamically increases with heavy load PSR. However, the utilization of many analog circuits obviously undermines the process scalability.

4. Discussion and conclusion

With the development of efficient computing and granular power management techniques, the DLDO has drawn sig-

nificant attention in recent years. When compared with its analog counterpart, the DLDO suits well the requirements of low voltage operation and process scalability. However, inferior performances in the transient response, recovery, and PSR prevent its further application. Previous works proposed partially address these issues. Alternatively, analog techniques complementary to the DLDO can improve the transient response and the PSR. Yet, the achieved PSR so far is still too low to supply analog or RF circuits.

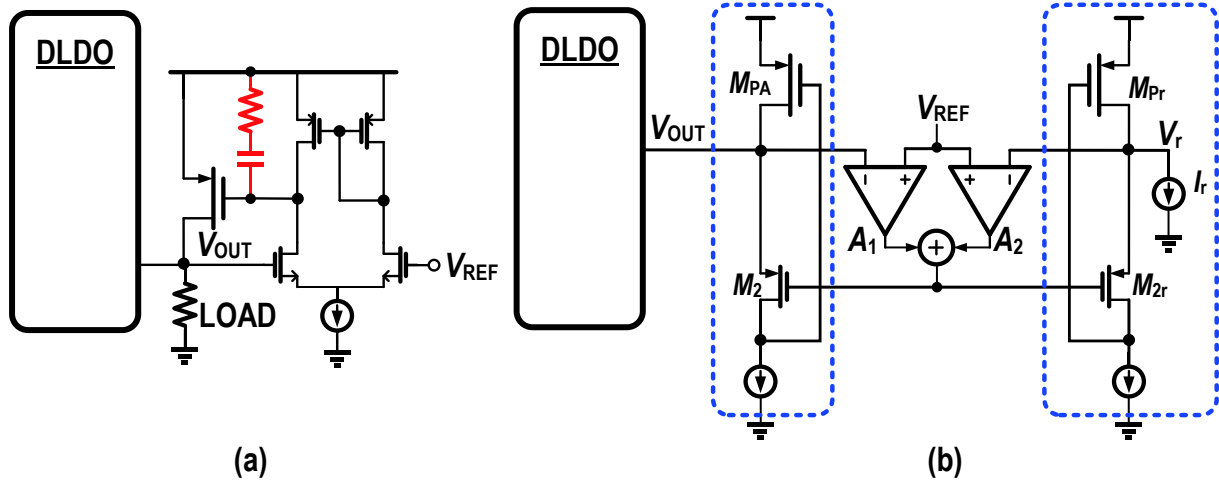


Fig. 14. Improving PSR using (a) feedforward PSR cancellation^[33] and (b) replica loop^[34, 35].

Table 2. FoM of speed versus process nodes.

Year	Process (nm)	Architecture	FoM (ps)
2020 ^[39]	130	ADC + PID	63.9
2016 ^[22]	65	ADC + Event driven	20
2016 ^[21]	28	ADC + Coarse/fine	9.57
2020 ^[40]	20	ADC + Computational	6.7
2020 ^[36]	10	TDC + PID	5.2
2017 ^[15]	65	Analog-assisted	0.23
2018 ^[18]	28	Analog-assisted	0.026

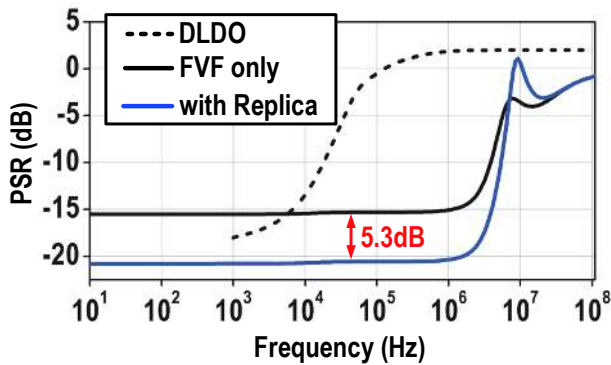


Fig. 15. (Color online) Simulated PSRs of the conventional DLDO, hybrid LDOs without replica loop, and with replica loop.

For the future design trends, it would not be easy for the DLDO to achieve a similar or even better performance than the ALDO, at circuit level. Instead, the performance should be significantly improved in the digital domain, or at the system-level. For instance, to maintain the stability and fast response, the PID coefficients were dynamically set in Ref. [39] through a digital calibration algorithm. Meanwhile, Ref. [40] proposed a computational scheme to determine the duration of the fully turn-on/turn-off power transistor array, for a very fast transient response. It would be possible to incorporate machine-learning techniques to predict, study, and respond to the load and supply changes. Moreover, fully synthesizable DLDOs^[36–38] are attractive with perfect compatibility to digital design flow and process scalability. Finally, it is interesting to investigate high current DLDOs with distributed layout and current sharing function. For instance, consider that some DLDOs in an SoC might not provide full load current in

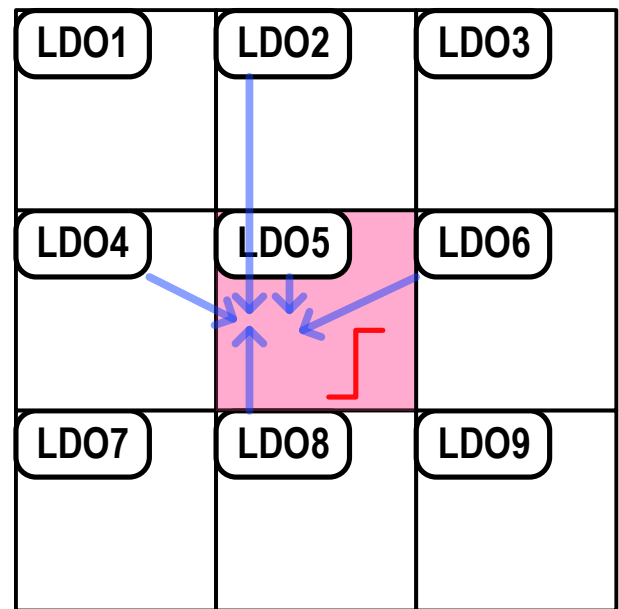


Fig. 16. (Color online) Multi-LDOs assisting a neighboring load step.

most workload scenarios, it is reasonable to make them to assist neighboring load steps^[41], as shown in Fig. 16. How to equalize the assisting currents may worth further studying.

Acknowledgements

This work was supported by the National Natural Science Foundation of China (No. 61974046), the Provincial Key Research and Development Program of Guangdong (2019B010140002), the Macao Science & Technology Development Fund (FDCT) 145/2019/A3 and SKL-AMSV(UM)-2020-2022.

References

- [1] Meinerzhagen P A, Tokunaga C, Malavasi A, et al. An energy-efficient graphics processor in 14-nm tri-gate CMOS featuring integrated voltage regulators for fine-grain DVFS, retentive sleep, and V_{MIN} optimization. *IEEE J Solid-State Circuits*, 2019, 54, 144
- [2] Nasir S B, Gangopadhyay S, Raychowdhury A. A 0.13 μm fully digital low-dropout regulator with adaptive control and reduced dynamic stability for ultra-wide dynamic range. 2015 IEEE International Solid-State Circuits Conference (ISSCC), 2015, 1

- [3] Chong S, Chan P K. A 0.9- μ A quiescent current output-capacitor-less LDO regulator with adaptive power transistors in 65-nm CMOS. *IEEE Trans Circuits Syst I*, 2013, 60, 1072
- [4] Lu Y, Wang Y P, Pan Q, et al. A fully-integrated low-dropout regulator with full-spectrum power supply rejection. *IEEE Trans Circuits Syst I*, 2015, 62, 707
- [5] Huang M, Feng H G, Lu Y. A fully integrated FVF-based low-dropout regulator with wide load capacitance and current ranges. *IEEE Trans Power Electron*, 2019, 34, 11880
- [6] Cai G G, Zhan C C, Lu Y. A fast-transient-response fully-integrated digital LDO with adaptive current step size control. 2019 IEEE Int Symp Circuits Syst ISCAS, 2019, 1
- [7] Park C J, Onabajo M, Silva-Martinez J. External capacitor-less low drop-out regulator with 25 dB superior power supply rejection in the 0.4–4 MHz range. *IEEE J Solid-State Circuits*, 2014, 49, 486
- [8] Lu Y, Martins R P, Seng-Pan U, et al. A 312 ps response-time LDO with enhanced super source follower in 28 nm CMOS. *Electron Lett*, 2016, 52, 1368
- [9] Gupta V, Rincon-Mora G A, Raha P. Analysis and design of monolithic, high PSR, linear regulators for SoC applications. IEEE International SOC Conference, 2004, 311
- [10] Okuma Y, Ishida K, Ryu Y, et al. 0.5-V input digital LDO with 98.7% current efficiency and 2.7- μ A quiescent current in 65 nm CMOS. IEEE Custom Integrated Circuits Conference, 2010, 1
- [11] Huang M, Lu Y, Sin S W, et al. Limit cycle oscillation reduction for digital low dropout regulators. *IEEE Trans Circuits Syst II*, 2016, 63, 903
- [12] Nasir S B, Raychowdhury A. On limit cycle oscillations in discrete-time digital linear regulators. 2015 IEEE Applied Power Electronics Conference and Exposition (APEC), 2015, 371
- [13] Huang M, Lu Y, Sin S W, et al. A fully integrated digital LDO with coarse-fine-tuning and burst-mode operation. *IEEE Trans Circuits Syst II*, 2016, 63, 683
- [14] Salem L G, Warchall J, Mercier P P. A successive approximation recursive digital low-dropout voltage regulator with PD compensation and sub-LSB duty control. *IEEE J Solid-State Circuits*, 2018, 53, 35
- [15] Huang M, Lu Y, Seng-Pan U, et al. An output-capacitor-free analog-assisted digital low-dropout regulator with tri-loop control. 2017 IEEE International Solid-State Circuits Conference (ISSCC), 2017, 342
- [16] Huang M, Lu Y, U S P, et al. An analog-assisted tri-loop digital low-dropout regulator. *IEEE J Solid-State Circuits*, 2018, 53, 20
- [17] Huang M, Lu Y, Lu X. Partial analogue-assisted digital low dropout regulator with transient body-drive and $2.5 \times$ FOM improvement. *Electron Lett*, 2018, 54, 282
- [18] Ma X F, Lu Y, Martins R P, et al. A 0.4 V 430 nA quiescent current NMOS digital LDO with NAND-based analog-assisted loop in 28 nm CMOS. 2018 IEEE International Solid-State Circuits Conference (ISSCC), 2018, 306
- [19] Akram M A, Hong W, Hwang I C. Fast transient fully standard-cell-based all digital low-dropout regulator with 99.97% current efficiency. *IEEE Trans Power Electron*, 2018, 33, 8011
- [20] Sun X, Boora A, Zhang W B, et al. A 0.6-to-1.1 V computationally regulated digital LDO with 2.79-cycle mean settling time and autonomous runtime gain tracking in 65 nm CMOS. 2019 IEEE International Solid-State Circuits Conference (ISSCC), 2019, 230
- [21] Lee Y J, Jung M Y, Singh S, et al. A 200 mA digital low-drop-out regulator with coarse-fine dual loop in mobile application processors. 2016 IEEE International Solid-State Circuits Conference (ISSCC), 2016, 150
- [22] Kim D, Seok M. Fully integrated low-drop-out regulator based on event-driven PI control. 2016 IEEE International Solid-State Circuits Conference (ISSCC), 2016, 148
- [23] Otsuga K, Onouchi M, Igarashi Y, et al. An on-chip 250 mA 40 nm CMOS digital LDO using dynamic sampling clock frequency scaling with offset-free TDC-based voltage sensor. 2012 IEEE International SOC Conference, 2012, 11
- [24] Gangopadhyay S, Somasekhar D, Tschanz J W, et al. A 32 nm embedded, fully-digital, phase-locked low dropout regulator for fine grained power management in digital circuits. *IEEE J Solid-State Circuits*, 2014, 49, 2684
- [25] Kundu S, Liu M Q, Wen S J, et al. A fully integrated digital LDO with built-in adaptive sampling and active voltage positioning using a beat-frequency quantizer. *IEEE J Solid-State Circuits*, 2019, 54, 109
- [26] Lee Y H, Peng S Y, Chiu C C, et al. A low quiescent current asynchronous digital-LDO with PLL-modulated fast-DVS power management in 40 nm SoC for MIPS performance improvement. *IEEE J Solid-State Circuits*, 2013, 48, 1018
- [27] Yang F, Mok P K T. A nanosecond-transient fine-grained digital LDO with multi-step switching scheme and asynchronous adaptive pipeline control. *IEEE J Solid-State Circuits*, 2017, 52, 2463
- [28] Lu Y, Huang M, Martins R P. PID control considerations for analog-digital hybrid low-dropout regulators. 2019 IEEE International Conference on Electron Devices and Solid-State Circuits (EDSSC), 2019, 1
- [29] Kim S T, Shih Y C, Mazumdar K, et al. Enabling wide autonomous DVFS in a 22 nm graphics execution core using a digitally controlled hybrid LDO/switched-capacitor VR with fast droop mitigation. 2015 IEEE International Solid-State Circuits Conference (ISSCC), 2015, 1
- [30] Zhang Y N, Song H X, Zhou R R, et al. A capacitor-less ripple-less hybrid LDO with exponential ratio array and 4000x load current range. *IEEE Trans Circuits Syst II*, 2019, 66, 36
- [31] Wang X Y, Mercier P P. A dynamically high-impedance charge-pump-based LDO with digital-LDO-like properties achieving a sub-4-fs FoM. *IEEE J Solid-State Circuits*, 2020, 55, 719
- [32] Nasir S B, Sen S, Raychowdhury A. Switched-mode-control based hybrid LDO for fine-grain power management of digital load circuits. *IEEE J Solid-State Circuits*, 2018, 53, 569
- [33] Liu X S, Krishnamurthy H K, Na T, et al. A modular hybrid LDO with fast load-transient response and programmable PSRR in 14 nm CMOS featuring dynamic clamp tuning and time-constant compensation. 2019 IEEE International Solid-State Circuits Conference (ISSCC), 2019, 234
- [34] Huang M, Lu Y. An analog-proportional digital-integral multi-loop digital LDO with fast response, improved PSR and zero minimum load current. 2019 IEEE Custom Integrated Circuits Conference (CICC), 2019, 1
- [35] Huang M, Lu Y, Martins R P. An analog-proportional digital-integral multiloop digital LDO with PSR improvement and LCO reduction. *IEEE J Solid-State Circuits*, 2020, 55, 1637
- [36] Bang S, Lim W, Augustine C, et al. A fully synthesizable distributed and scalable all-digital LDO in 10 nm CMOS. 2020 IEEE International Solid-State Circuits Conference (ISSCC), 2020, 380
- [37] Li Y F, Zhang X Y, Zhang Z, et al. A 0.45-to-1.2-V fully digital low-dropout voltage regulator with fast-transient controller for near/subthreshold circuits. *IEEE Trans Power Electron*, 2016, 31, 6341
- [38] Oh J, Park J E, Hwang Y H, et al. A 480 mA output-capacitor-free synthesizable digital LDO using CMP-triggered oscillator and droop detector with 99.99% current efficiency, 1.3 ns response time, and 9.8 A/mm² current density. 2020 IEEE International Solid-State Circuits Conference (ISSCC), 2020, 382
- [39] Singh A, Kar M, Chekuri V C K, et al. A digital low-dropout regulator with autotuned PID compensator and dynamic gain control for improved transient performance under process variations and aging. *IEEE Trans Power Electron*, 2020, 35, 3242
- [40] Ahmed K Z, Krishnamurthy H K, Augustine C, et al. A variation-adaptive integrated computational digital LDO in 22-nm CMOS with fast transient response. *IEEE J Solid-State Circuits*, 2020, 55,

977

- [41] Lu Y, Yang F, Chen F, et al. A 500 mA analog-assisted digital-LDO-based on-chip distributed power delivery grid with cooperative regulation and IR-drop reduction in 65 nm CMOS. 2018 IEEE International Solid-State Circuits Conference (ISSCC), 2018, 310
- [42] Hershberg B, Weaver S, Sobue K, et al. Ring amplifiers for switched capacitor circuits. *IEEE J Solid-State Circuits*, 2012, 47, 2928
- [43] Yang F, Mok P K T. A 65 nm inverter-based low-dropout regulator with rail-to-rail regulation and over -20 dB PSR at 0.2 V lowest supply voltage. 2017 IEEE International Solid-State Circuits Conference (ISSCC), 2017, 106
- [44] Park J E, Hwang J, Oh J, et al. A 0.4-to-1.2 V 0.0057 mm² 55fs-transient-FoM ring-amplifier-based low-dropout regulator with replica-based PSR enhancement. 2020 IEEE International Solid-State Circuits Conference (ISSCC), 2020, 492
- [45] Hazucha P, Karnik T, Bloechel B A, et al. Area-efficient linear regulator with ultra-fast load regulation. *IEEE J Solid-State Circuits*, 2005, 40, 933
- [46] Duong Q H, Nguyen H H, Kong J W, et al. Multiple-loop design technique for high-performance low-dropout regulator. *IEEE J Solid-State Circuits*, 2017, 52, 2533